Available online at www.sciencedirect.com

SciVerse ScienceDirect

Journal of the European Ceramic Society 32 (2012) 947–954

www.elsevier.com/locate/jeurceramsoc

Oxidation of ZrC–30 vol% SiC composite in air from low to ultrahigh temperature

Liyou Zhao, Dechang Jia*, Xiaoming Duan, Zhihua Yang, Yu Zhou

Institute for Advanced Ceramics, Harbin Institute of Technology, Harbin 150080, China

Received 3 May 2011; received in revised form 13 October 2011; accepted 17 October 2011
Available online 8 November 2011

Abstract

Oxidation of ZrC–30 vol.% SiC is investigated in air using furnace and oxyacetylene torch. The microstructure and phase composition of oxide scales are analyzed via SEM, XRD, and Raman. At 800 and 1100 °C, SiC is embedded in the porous and cracked ZrO_2 scales, which have a single-layer structure and are almost non-protective. At 1300 and 1500 °C, the protective effect of oxide scales is enhanced by the formed SiO_2. The scales consist of two subscales, outer and inner layers, during oxidation at 1300 °C for $\geq$1 h, and 1500 °C for $\geq$15 min. The growth kinetics of both layers is analyzed. At ~1700 °C, a new layer is observed between the outer and inner layers, which should contain less carbon than the inner layer. At ~2100 °C, the oxide scale is porous and contains many big holes. This scale shows a single-layer structure, which mainly consists of ZrO_2.

© 2011 Elsevier Ltd. All rights reserved.

Keywords: A. Hot pressing; D. Carbides; D. SiC; D. Carbon; Oxidation

1. Introduction

Interest in ultrahigh-temperature ceramics (UHTCs) has increased significantly in recent years due to the drive to produce a thermal protection system and other components for hypersonic aerospace vehicles.[1–3] Zirconium carbide (ZrC) is an important member of UHTCs. Besides its high melting temperature, ZrC has a unique combination of high fracture strength, high electrical and thermal conductivity, and resistance to erosion/corrosion.[4–6]

Oxidation resistance is a major issue in the development of UHTCs, but ZrC has a poor high-temperature chemical stability in oxidizing atmosphere, which significantly limits its actual application as UHTCs. Previous reports indicated that ZrO_2 scales on ZrC can be divided into two layers.[7–12] The outer layer is porous and cracked, containing a small amount of free carbon. Pores and cracks in the outer layer offer channels for inward diffusion of oxygen. So, the outer layer is non-protective. The inner layer is relatively dense and rich in carbon, which attracts lots of attention in the past several years. This layer is considered as a barrier for the diffusion of oxygen during oxidation. However, the inner layer is very thin; that is to say, oxide scale on ZrC mainly consists of the porous and cracked outer layer. Cracks in the outer layer penetrate easily into the inner layer, accelerating the oxidation of matrix. So, the oxide scale on ZrC is almost non-protective, which is confirmed by the linear or approximately linear oxidation kinetics.[7,9,13,14]

A common approach to improve oxidation resistance of UHTCs is the incorporation of Si-containing compounds into UHTCs matrix to form a protective SiO_2-containing oxide scale.[15–18] However, the reports are scarce by far on oxidation of ZrC-based composites with additives of Si-containing compounds, and some results deviate from that expected. Pierrat et al.[19] investigated the oxidation resistance of pressureless-sintered ZrC–20 vol.% $MoSi_2$ using an experimental facility called REHPTS. The results showed that addition of 20 vol.% $MoSi_2$ was detrimental to the oxidation behavior of ZrC in the temperature range of 1800–2400 K, because of its dissociation and its role in the surface melting. Li et al.[20] prepared a ZrC–SiC coating on 2D C/ZrC–SiC composites by chemical vapor deposition and investigated the oxidation behavior of this composites at 1800 °C using CH_4 combustion wind tunnel. The results

---

* Corresponding author. Tel.: +86 451 86418792; fax: +86 451 86414291.
E-mail addresses: dcjia@hit.edu.cn, dechangjia@yahoo.com (D. Jia).

0955-2219/$ – see front matter © 2011 Elsevier Ltd. All rights reserved.
doi:10.1016/j.jeurceramsoc.2011.10.024

indicated that no protective oxide scale was formed, because ZrC was oxidized completely very fast, and SiC or its oxide SiO_2 was easily blown off. Zhao et al.[21] prepared C/ZrC–SiC by polymer infiltration and pyrolysis process. Furnace test at 1200 °C in air indicated that introduction of 1.9 vol.% SiC can improve the oxidation resistance of C/ZrC, due to formation of dense SiO_2 glass.

In this study, we investigated the oxidation behavior of hot-pressed ZrC–30 vol.% SiC in air from low to ultrahigh temperature using furnace and oxyacetylene torch. The structure evolution of oxide scales was described and discussed. Some interesting phenomena were reported which have not been found in previous works.

2. Material and methods

ZrC–30 vol.% SiC composite was referred as ZrC–30SiC below. The starting powders were ZrC (mean particle size 2.1 μm, >98% purity, Changsha Wing High High-Tech New Materials Co., Ltd., China), SiC (β-SiC, mean particle size 2 μm, >99% purity, Central Iron & Steel Research Institute, China). The powder mixture of ZrC–30 vol.% SiC was ball milled in ethanol for 24 h and then dried. Mixed powders were then uniaxially hot pressed in boron nitride-coated graphite die at 2000 °C for 60 min under an argon atmosphere with an applied pressure of 30 MPa. Bulk density and theoretical density were evaluated using the Archimedes method and the rule of mixtures, respectively. Sample coupons in the size of 4.9 mm × 5.8 mm × 6.6 mm were cut from the hot-pressed specimens, and all surfaces were diamond polished to a 1 μm finish. Coupons were ultrasonically cleaned in acetone and alcohol, and then exposed to air at temperature of 800, 1100, 1300 and 1500 °C, respectively, for 15 min to 4 h. The oxidation experiment was conducted in a box furnace with $MoSi_2$ heating elements. The weight of samples before and after oxidation was carefully measured using a precision balance with an accuracy of 10^{-5} g. Sample coupons with dimension of $\Phi 17.4 \times 12.7$ mm were used in the oxidation experiment at temperature of ∼1700 and ∼2100 °C, which was carried out with the oxyacetylene torch facility of Hu et al.'s group.[22,23] The oxyacetylene torch test was conducted under two different conditions. During the first test, after several adjustments of gas flow rate, the pressure and flux of acetylene were fixed at 0.1 MPa and 0.32 $m^3\,h^{-1}$, and for oxygen 0.5 MPa and 0.64 $m^3\,h^{-1}$, respectively. The test time was about 13 min. The sample surface achieves a temperature of 1670 °C within about 3 min, and then it gradually increases to 1700 °C. During the second test, the pressure and flux of acetylene were 0.1 MPa and 0.75 $m^3\,h^{-1}$, and for oxygen 0.5 MPa and 1.5 $m^3\,h^{-1}$, respectively. The test time was about 10 min. The temperature of sample surface increases sharply to 2060 °C and then gradually reaches to the maximal value of 2200 °C. The phase composition of oxide scale was identified using X-ray diffractometer and Raman spectroscopy. X-ray diffraction (XRD) was carried out in a D/max-2200VPC diffractometer (Rigaku, Tokyo, Japan) with Cu Kα radiation. The Raman spectra were recorded using the 458 nm line from an argon ion laser using a Raman system (JY HR800, Paris, France). The surface and cross section of oxidized samples were observed by scanning electron microscope (SEM, FEI Quanta 200F, Eindhoven, the Netherlands). An optical microscope (Axiovert 40MAT, Germany) was also employed to observe the cross section of oxide scale and determine its thickness.

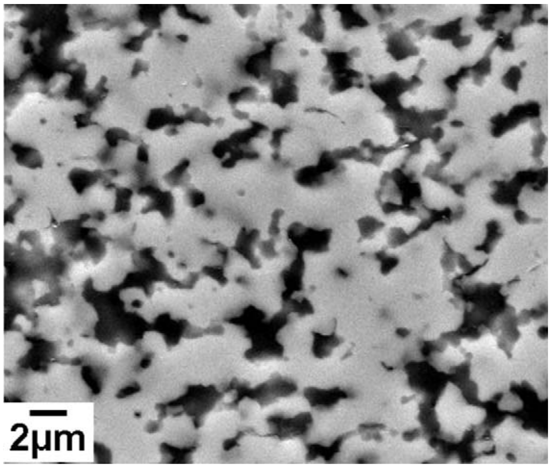

Fig. 1. SEM micrograph of the polished surface of ZrC–30SiC.

3. Results

3.1. Density and microstructure

The measured bulk density of ZrC–30SiC is 5.56 g/cm^3, which corresponds to a relative density of 98.4%. Fig. 1 shows a SEM micrograph of the polished surface of ZrC–30SiC. The dark and grey phases are SiC, and they appear to be uniformly dispersed in the light ZrC matrix. The different contrast of SiC should be related to their different crystallographic orientations.[24,25] Microstructure of the composite is regular, and few pores are observed on the polished surface, which supports the result of density measurement.

3.2. Oxidation at low temperature range (800 and 1100 °C)

XRD analysis (Fig. 2a) indicates that the oxide scale formed at 1100 °C for 15 min consists of m-ZrO_2. Fig. 3a shows the surface SEM micrograph of this scale. It is cracked and porous. SiC is embedded in ZrO_2. Because the strongest peak of SiC (1 1 1) at 35.6° and the peaks of m-ZrO_2 (2 0 0) at 35.3°, $(\bar{1}\ 0\ 2)$ at 35.9° are too close to be distinguished, SiC is difficult to detect by XRD in m-ZrO_2 matrix. Cross-section SEM micrograph (Fig. 3b) indicates that the oxide scale has a single-layer structure. Its thickness is about 290 μm, and mass gain of sample is 177.9 g/m^2. Fig. 4 shows the Raman spectrum of this scale. Two broad peaks appear around 1350 cm^{-1} and 1600 cm^{-1}, corresponding to the A_{1g} mode associated with amorphous carbon and E_{2g} with graphite, respectively.[8] Fig. 5 shows the specific mass-change as a function of exposure time for ZrC–30SiC during oxidation at 800 and 1100 °C. The kinetics follows an approximately linear law, indicating that the oxidation proceeds mainly via interface limited reaction.

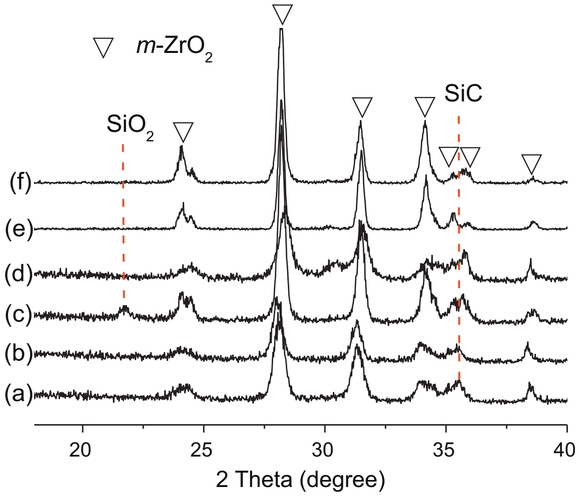

Fig. 2. XRD patterns of the oxide scale on ZrC–30SiC: (a) 1100 °C for 15 min, (b) 1300 °C for 15 min, (c) outer layer at 1500 °C for 15 min, (d) inner layer at 1500 °C for 15 min, (e) the first oxyacetylene torch test (∼1700 °C) and (f) the second oxyacetylene torch test (∼2100 °C).

3.3. Oxidation at intermediate temperature range (1300 and 1500 °C)

Microstructure and phase composition of the oxide scale formed at 1300 °C for 15 min are similar to that of scale formed at 1100 °C for 15 min. No SiO_2 is detected on the surface of oxidized sample by XRD (Fig. 2b) and SEM (Fig. 6a). The oxide scale shows a single-layer structure (Fig. 6b). The thickness of this scale is about 295 μm; mass gain of sample is 179.8 g/m^2. After oxidation at 1500 °C for 15 min, most SiC on the surface of sample oxidizes to form SiO_2 (Fig. 6c). The oxide scale shows a duplex structure (Fig. 6d). The thickness of this scale is about 300 μm, and mass gain of sample is 181.6 g/m^2. High magnification micrographs indicate that, the outer layer contains some pores, and the grey SiO_2 mainly distributes in these pores; the inner layer appears to be dense, and SiC is almost not oxidized in the inner layer. For further analyzing the phase composition, each layer of scale was separated from sample. The outer layer is white in color. XRD pattern (Fig. 2c) reveals that it consists of m-ZrO_2 and SiO_2. Raman spectrum analysis, shown in Fig. 7a, indicates presence of some free carbon in the outer layer. The Raman shifts between 100 and 1000 cm^{-1} are characteristic peaks for m-ZrO_2 and possibly SiO_2.[26,27] The inner layer is black in color. XRD pattern (Fig. 2d) reveals that

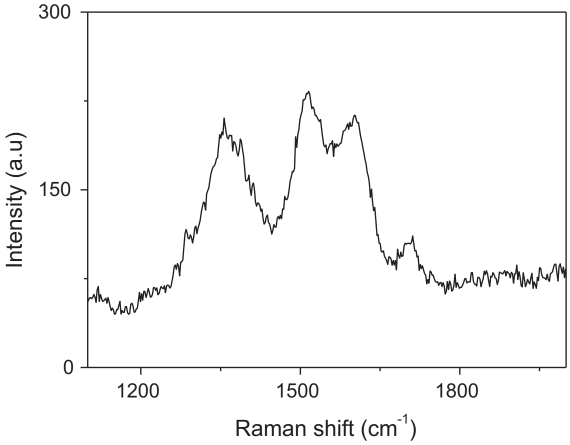

Fig. 4. Raman spectrum of the oxide scale on ZrC–30SiC oxidized at 1100 °C for 15 min.

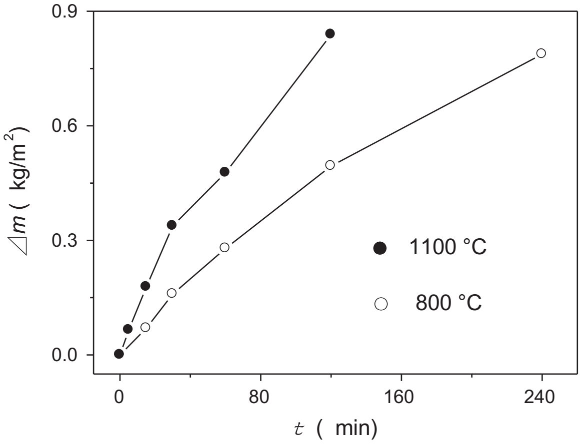

Fig. 5. Specific mass-change (Δm) as a function of exposure time (t) for ZrC–30SiC during oxidation at 800 and 1100 °C.

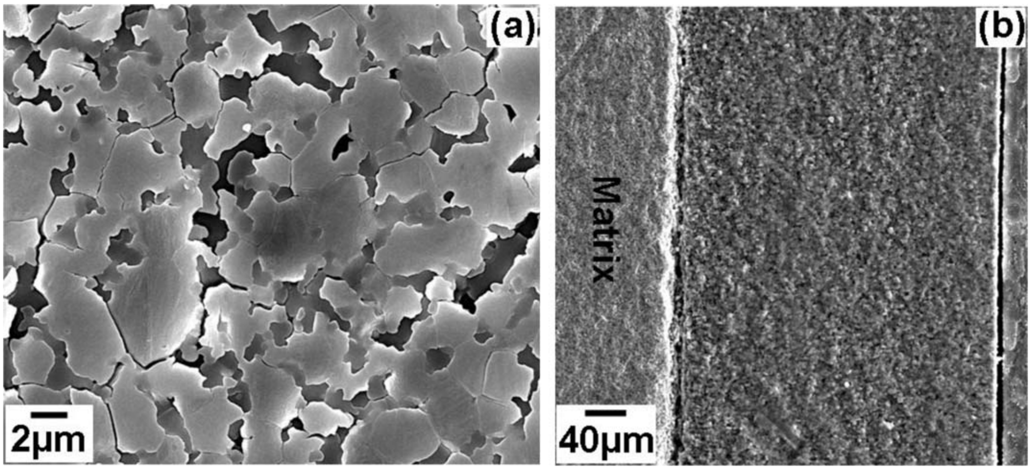

Fig. 3. Surface (a) and cross-section (b) SEM micrographs of ZrC–30SiC oxidized at 1100 °C for 15 min.

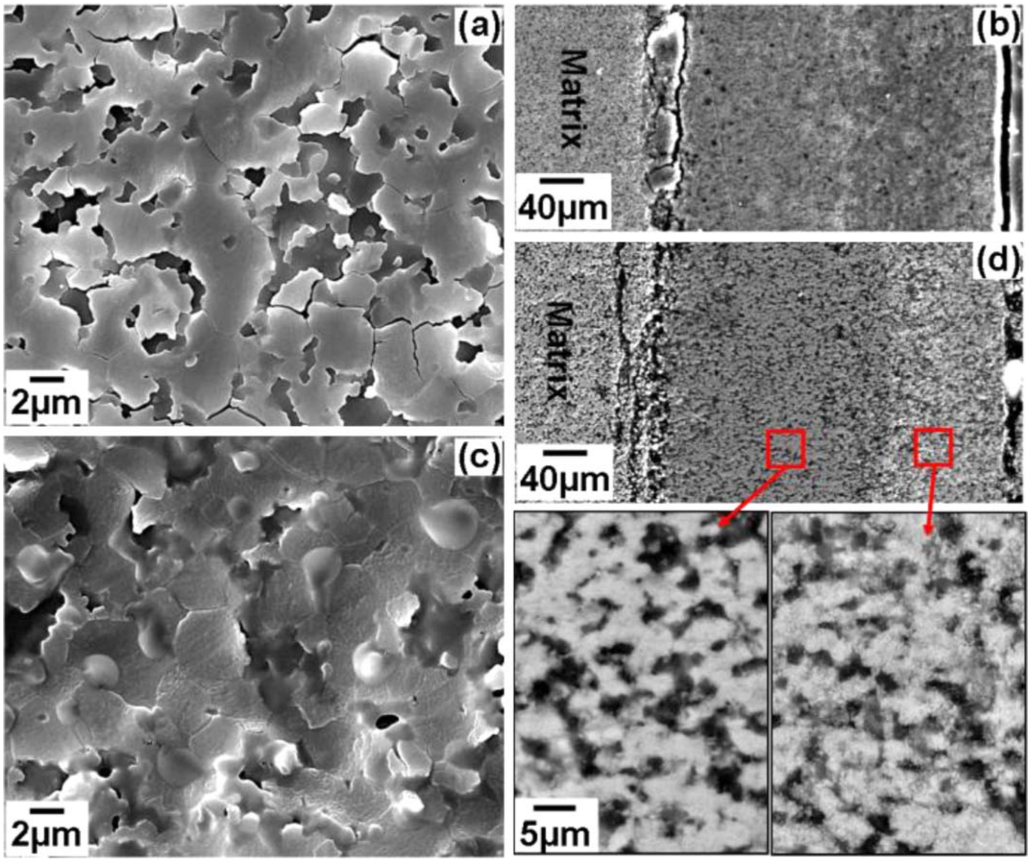

Fig. 6. Surface and cross-section SEM micrographs of ZrC–30SiC oxidized at 1300 (a and b) and 1500 °C (c and d) for 15 min.

the matrix of inner layer is composed of m-ZrO_2. Raman spectrum of inner layer (Fig. 7b) shows much bigger intensity ratio of the peaks for free carbon to the peaks for m-ZrO_2 than the spectrum of outer layer, indicating that the inner layer contains more free carbon. Similar duplex-structure scales are found during oxidation of ZrC–30SiC at 1300 °C for $\geq$1 h, and 1500 °C for $\geq$15 min.

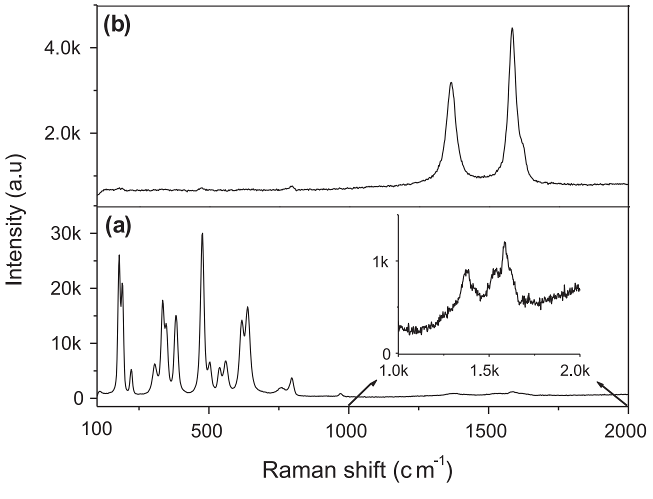

Fig. 7. Raman spectra for the outer (a) and inner (b) layers of oxide scale on ZrC–30SiC oxidized at 1100 °C for 15 min.

The time dependency of thickness of the inner and outer layers during oxidation at 1300 and 1500 °C is shown in Fig. 8. At both temperatures, the thickness of outer layer almost does not change with time after forming duplex structure, while the thickening of inner layer is approximately parabolic with time. The outer layer is thicker at 1300 °C than at 1500 °C.

Fig. 9 shows the specific mass-change and its corresponding square as a function of exposure time for ZrC–30SiC during oxidation at 1300 and 1500 °C. The kinetics is in approximate agreement with parabolic law, indicating that the oxidation is mainly controlled by diffusion. Fig. 10 shows the optical macrograph of ZrC and ZrC–30SiC oxidized at 1300 and 1500 °C for 15 min. We can see that the ZrC samples are oxidized catastrophically while the oxidation of ZrC–30SiC is not so serious. ZrC–30SiC has a better oxidation resistance than ZrC in air at 1300 and 1500 °C.

3.4. Oxidation at high and ultrahigh temperature (about 1700 and 2100 °C)

Fig. 11a shows a surface SEM micrograph of the scale on sample after the first oxyacetylene torch test ($\sim$1700 °C). Many pores and a small amount of SiO_2 are observed. SiO_2 is too little to be detected by XRD (Fig. 2e). Low magnification SEM micrograph (Fig. 11b) indicates that the cross-section morphology of this scale is similar to that of scale formed at 1500 °C for 15 min, except formation of an interlayer between the outer

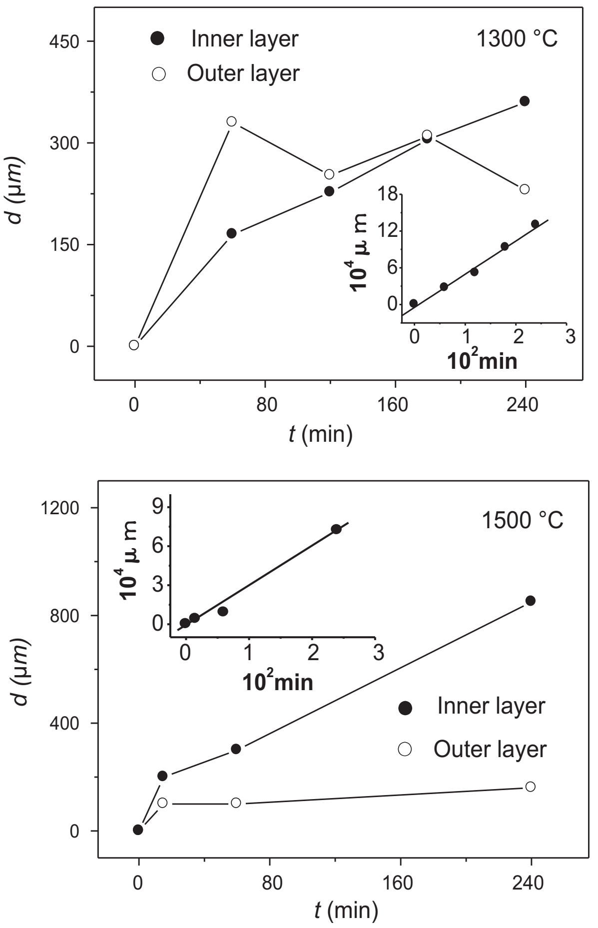

Fig. 8. Time (*t*) dependency of the thickness (*d*) of inner and outer layers during oxidation at 1300 and 1500 °C. The inset is the plot of d^2 vs *t* for the data of inner layer.

and inner layers. Porosity and color (Fig. 11c) of the interlayer are intermediate between that of the outer and inner layers. The thickness of oxide scale is about 220 μm. High magnification micrographs indicate that, both inner layer and interlayer are mainly composed of ZrO_2 and SiC; the amount of SiO_2 in the outer layer is decreased, and porosity increased, compared with that of the outer layer during oxidation at 1500 °C for 15 min. Based on the analysis in Section 3.3, it can be inferred that the carbon content of interlayer is lower than that of inner layer, but higher than that of outer layer. After the second oxyacetylene torch test (~2100 °C), many macroscopic holes are present on the surface of scale, and this scale mainly consists of *m*-ZrO_2 (Fig. 2f). Surface SEM micrograph (Fig. 11d) shows three different regions, namely, porous ZrO_2 skeleton, big holes, and a little SiO_2. This scale has a single-layer structure (Fig. 11e), and its thickness is about 350 μm.

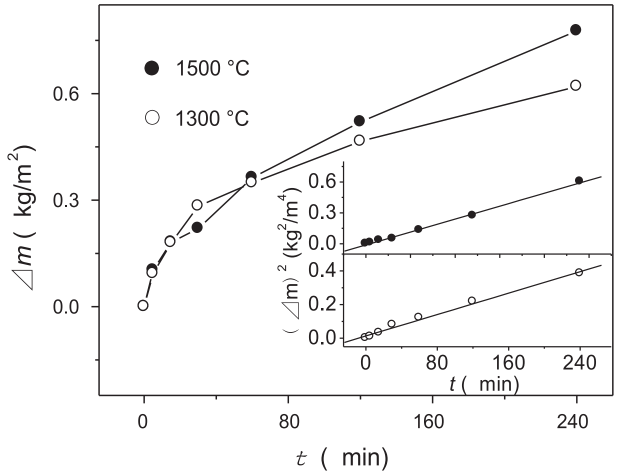

Fig. 9. Specific mass-change (Δ*m*) and its corresponding square (inset) as a function of exposure time (*t*) for ZrC–30SiC during oxidation at 1300 and 1500 °C.

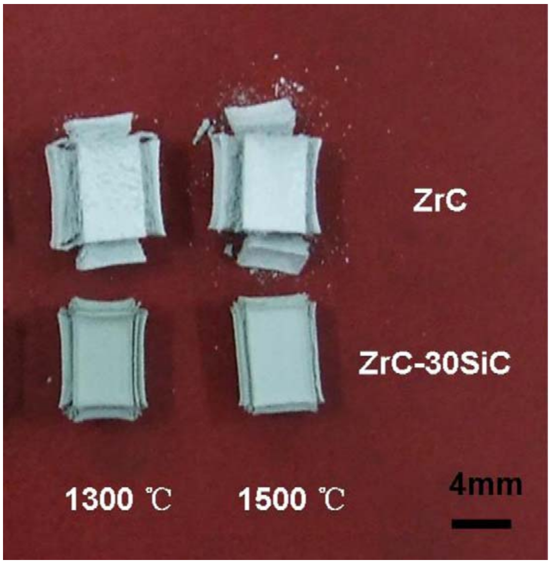

Fig. 10. Optical macrograph of ZrC and ZrC–30SiC oxidized at 1300 and 1500 °C for 15 min.

4. Discussion

We know that one of the differences between the two layers of oxide scales on ZrC–30SiC is the higher carbon content of inner layer, which is consistent with the previous reports on oxidation of ZrC. During XRD analysis, no obvious ZrO_2 peak shift is observed in the pattern of inner layer when compared with that of outer layer, but we do not exclude the possibility of presence of reported oxycarbide ($ZrO_{2-x}C_y$ here) in the inner layer.[28,29] Carbon is easy to burn out in air at high temperature, whether in the lattice of $ZrO_{2-x}C_y$ or as a simple substance.[30–32] So, it depends on the protective effect of oxide scales whether the inner layer appears. Oxidation rate of SiC is negligible below 1100 °C in air.[30] Oxidation behavior of ZrC–30SiC should be similar to that of ZrC at this temperature range. Generally, dense ZrC ceramic oxidizes remarkably at 800 °C in air,[7] and the oxidation by reaction (1) is thermodynamically the most probable.[33]

$$ZrC(s) + O_2(g) = ZrO_2(s) + C(s) \qquad (1)$$

The porous and cracked oxide scales are almost non-protective during oxidation at 800 and 1100 °C. Most of the formed carbon would be oxidized to generate gases CO_2 and CO. The oxide scales show a single layer structure. Because

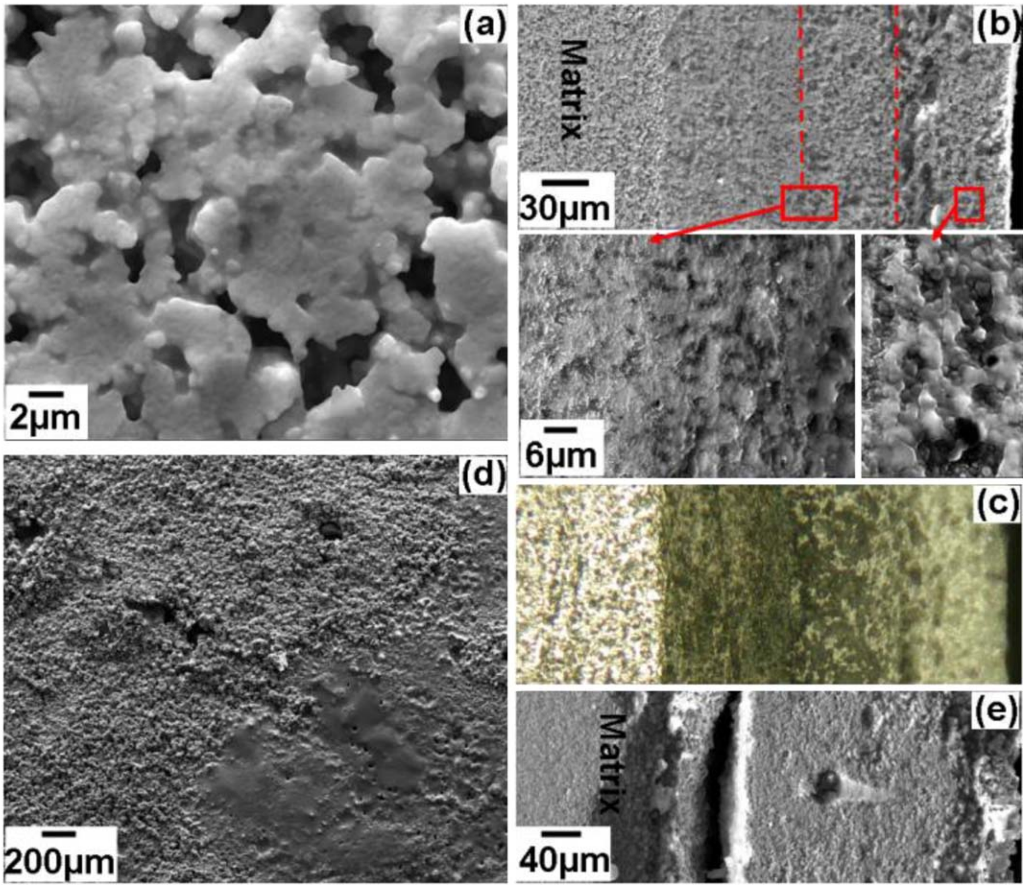

Fig. 11. Surface and cross-section SEM micrographs of ZrC–30SiC after the first (~1700 °C, a and b) and second (~2100 °C, d and e) oxyacetylene torch test. (c) Shows a corresponding optical micrograph of (b).

diffusion of CO_2 and CO through ZrO_2 is difficult,[9] a small amount of carbon remains in the scale. SiC starts to oxidize significantly at 1300 °C.[34] The formed SiO_2 could seal the pores and cracks of scales, increasing the density of scales thus retarding inward diffusion of oxygen. However, the oxide scale formed at 1300 °C for 15 min still can not protect most of the formed carbon from oxidation, because the exposure time is too short to generate enough SiO_2. In contrast, during oxidation at 1500 °C for 15 min, more SiO_2 is formed due to the more rapid oxidation of SiC. The local oxygen concentration in the regions of the matrix/scale interface becomes so low that a carbon-rich ZrO_2 layer is formed, i.e., the observed black inner layer of scale.

Growth process of each layer of scales on ZrC–30SiC during oxidation at 1300 and 1500 °C can be described as follows. ZrC oxidizes quickly to form a porous ZrO_2 scale, i.e., the outer layer. The thickness of outer layer increases with time. SiC oxidizes relatively slowly to form SiO_2 and enhances the protective effect of outer layer. As the inner layer forms, the outer layer stops thickening and the inner layer thickens with time. Oxidation rate of SiC is relatively lower at 1300 °C. So, the inner layer appears later, and the outer layer is thicker. As mentioned above, carbon is chemically unstable in air at high temperature. The outer layer of scales is relatively porous. However, why doesn't the carbon of inner layer near the interface of two layers oxidize gradually to result in thickening of outer layer? A rational conjecture is that, the formed carbon diffuses outward and reacts with oxygen in the outer layer; also, oxidation of carbon is slower than diffusion. Outward diffusion of carbon has been observed during oxidation of ZrC and other carbides.[7,35,36] The outer layer of scales on ZrC–30SiC is protective, which can lower the oxidation rate of carbon. During oxidation, lots of inward diffused oxygen is consumed in the outer layer by reaction with outward diffused carbon. Due to the sufficient carbon from inner layer, the interface between inner and outer layers can not move inward. Zr is thermodynamically oxidized more easily than carbon.[33] Some oxygen diffuses through the inner layer to react with ZrC–30SiC matrix, resulting in thickening of the inner layer. Previous reports indicated that the porous outer layer thickens linearly with time, while the dense inner layer parabolically and then attains a limited constant thickness during oxidation of ZrC and other refractory carbides at low oxygen pressure.[9,37] The amount of carbon created at ZrC matrix/scale interface decreases with increasing of oxygen pressure.[38] So, the inner layer of oxide scale is usually difficult to observe during oxidation of ZrC in air.[7,14,39] In this study, ZrC forms a non-adherent oxide scale below 1500 °C which is brittle to touch, as Fig. 10 shows, and we do not find obvious duplex structure in them. Introduction of SiC enhances the protective effect of outer layer of scales on ZrC, promotes formation of the dense inner layer, and increases the volume ratio of inner layer to outer layer, therefore improving the oxidation resistance of ZrC in air at intermediate temperature range.

SiC starts to oxidize actively at 1650 °C according to reaction (2).[40]

$$SiC(s) + O_2(g) = SiO(g) + CO(g) \quad (2)$$

The amount of SiO_2 in the scale on ZrC–30SiC would decrease with increasing of oxidation temperature.[23,34,41] During the first oxyacetylene torch test (∼1700 °C), lots of gas products can be generated due to the serious oxidation of ZrC and active oxidation of SiC, which leave behind many pores after passing through oxide scale. The protective effect of outer layer of oxide scale will be weakened. So, we assume that some carbon of inner layer in the regions near outer layer is oxidized, resulting in formation of a new layer with higher porosity and lighter color than the inner layer. During the second oxyacetylene torch test (∼2100 °C), more gas products can be generated, which accelerates the damage of oxide scale, resulting in oxidation of the most formed carbon. The temperature under oxide scale is believed to be lower than the surface temperature. Part of SiC oxidizes passively to form SiO_2, which is beneficial to enhancing the oxidation resistance of ZrC.

5. Conclusions

Oxidation of ZrC–30 vol% SiC is studied in air. At 800 and 1100 °C, the porous and cracked scales are almost nonprotective, and exhibit a single-layer structure. These scales consist of ZrO_2, SiC, and a small mount of carbon. At 1300 and 1500 °C, SiO_2 enhances the protective effect of ZrO_2 scales. The ZrO_2 scales show a duplex structure during oxidation at 1300 °C for $\geq$1 h, and 1500 °C for $\geq$15 min. The outer layer is white and relatively porous, containing SiO_2 and less carbon; the inner layer is black and dense, containing SiC and more carbon. After forming duplex structure, the thickness of outer layer does not change with time, while the thickening of inner layer is approximately parabolic with time. At ∼1700 °C, an interlayer is observed between the outer and inner layers of scale, which should contain less carbon than the inner layer. At ∼2100 °C, the oxide scale is porous and contains many big holes. This scale shows a single-layer structure, and mainly consists of ZrO_2.

Acknowledgements

This work was supported by the Program for Changjiang Scholars and by the National Natural Science Foundation of China under grant No. 51021002.

References

1. Opeka MM, Talmy IG, Zaykoski JA. Oxidation-based materials selection for 2000 °C + hypersonic aerosurfaces: theoretical considerations and historical experience. *J Mater Sci* 2004;**39**:5887–904.
2. Levine SR, Opila EJ, Halbig MC, Kiser JD, Singh M, Salem JA. Evaluation of ultra-high temperature ceramics for aeropropulsion use. *J Eur Ceram Soc* 2002;**22**:2757–67.
3. Zou LH, Wali N, Yang J-M, Bansal NP. Microstructural development of a C_f/ZrC composite manufactured by reactive melt infiltration. *J Eur Ceram Soc* 2010;**30**:1527–35.
4. Pierson HO. *Handbook of refractory carbides and nitrides: properties, characteristics, processing, and application*. Westwood, NJ: Noyes publications; 1996.
5. Opeka MM, Talmy IG, Wuchina EJ, Zaykoski JA, Causey SJ. Mechanical, thermal, and oxidation properties of refractory hafnium and zirconium compounds. *J Eur Ceram Soc* 1999;**19**:2405–14.
6. Krajewski A, D'Alessio L, De Maria G. Physico-chemical and thermophysical properties of cubic binary carbides. *Cryst Res Technol* 1998;**33**:341–74.
7. Voitovich RF, Pugach EA. High-temperature oxidation of ZrC and HfC. *Powder Metall Met Ceram* 1973;**12**:916–21.
8. Shimada S, Yoshimatsu M, Inagaki M, Otani S. Formation and characterization of carbon at the ZrC/ZrO_2 interface by oxidation of ZrC single crystals. *Carbon* 1998;**36**:1125–31.
9. Shimada S, Nishisako M, Inagaki M. Formation and microstructure of carbon-containing oxide scales by oxidation of single crystals of zirconium carbide. *J Am Ceram Soc* 1995;**78**:41–8.
10. Shimada S, Inagaki M, Suzuki M. Microstructure observation of the ZrC/ZrO_2 interface formed by oxidation of ZrC. *J Mater Res* 1996;**11**:2594–7.
11. Shimada S. Interfacial reaction on oxidation of carbides with formation of carbon. *Solid State Ionics* 2001;**141–142**:99–104.
12. Shimada S. Microstructural observation of ZrO_2 scales formed by oxidation of ZrC single crystals with formation of carbon. *Solid State Ionics* 1997;**101–103**:749–53.
13. Berkowitz-Mattuck JB. High temperature oxidation IV. Zirconium and hafnium carbides. *J Electrochem Soc* 1964;**114**:1030–3.
14. Kuriakose AK, Margrave JL. The oxidation kinetics of zirconium diboride and zirconium carbide at high temperatures. *J Electrochem Soc* 1964;**111**:827–31.
15. Hu P, Wang GL, Wang Z. Oxidation mechanism and resistance of ZrB_2–SiC composites. *Corros Sci* 2009;**51**:2724–32.
16. Sciti D, Guicciardi S, Nygren M. Spark plasma sintering and mechanical behaviour of ZrC-based composites. *Scripta Mater* 2008;**59**:638–41.
17. Wang Z, Wu Z, Shi G. The oxidation behaviors of a ZrB_2–SiC–ZrC ceramic. *Solid State Sci* 2011;**13**:534–8.
18. Talmy IG, Zaykoski JA, Opeka MM, Smith AH. Properties of ceramics in the system ZrB_2–Ta_5Si_3. *J Mater Res* 2006;**21**:2593–9.
19. Pierrat B, Balat-Pichelin M, Silvestroni L, Sciti D. High temperature oxidation of ZrC–20% $MoSi_2$ in air for future solar receivers. *Sol Energy Mater Sol Cells* 2011;**95**:2228–37.
20. Li HB, Zhang LT, Cheng LF, Wang YG. Oxidation analysis of 2D C/ZrC–SiC composites with different coating structures in CH_4 combustion gas environment. *Ceram Int* 2009;**35**:2277–82.
21. Zhao D, Zhang CR, Hu HF, Zhang YD, Wang QK, He XB. Effect of SiC on the oxidation resistance performance of C/ZrC composite prepared by polymer infiltration and pyrolysis process. *Mater Sci Forum* 2011;**675-677**:415–8.
22. Zhou SB, Li WJ, Hu P, Hong CQ, Weng L. Ablation behavior of ZrB_2–SiC–ZrO_2 ceramic composites by means of the oxyacetylene torch. *Corros Sci* 2009;**51**:2071–9.
23. Han JC, Hu P, Zhang XH, Meng SH, Han WB. Oxidation-resistant ZrB_2–SiC composites at 2200 °C. *Compos Sci Technol* 2008;**68**:799–806.
24. Sciti D, Brach M, Bellosi A. Long-term oxidation behavior and mechanical strength degradation of a pressurelessly sintered ZrB_2–$MoSi_2$ ceramic. *Scripta Mater* 2005;**53**:1297–302.
25. Ni D-W, Zhang G-J, Xu F-F, Guo W-M. Initial stage of oxidation process and microstructure analysis of HfB_2–20 vol.% SiC composite at 1500 °C. *Scripta Mater* 2011;**64**:617–20.
26. Djurado E, Bouvier P, Lucazeau G. Crystallite size effect on the tetragonal-monoclinic transition of undoped nanocrystalline zirconia studied by XRD and Raman spectrometry. *J Solid State Chem* 2000;**149**:399–407.
27. Berry FJ, Skinner SJ, Bell IM, Clark RJH, Ponton CB. The influence of pH on zirconia formed from zirconium (IV) acetate solution: characterization by X-ray powder diffraction and Raman spectroscopy. *J Solid State Chem* 1999;**145**:394–400.

28. Bargeron CB, Benson RC. X-ray microanalysis of a hafnium carbide film oxidized at high temperature. *Surf Coat Technol* 1988;**36**:111–5.
29. Bargeron CB, Benson RC, Jette AN, Phillips TE. Oxidation of hafnium carbide in the temperature range 1400–2060 °C. *J Am Ceram Soc* 1993;**76**:1040–6.
30. Fahrenholtz WG. Thermodynamic analysis of ZrB_2–SiC oxidation: formation of a SiC-depleted region. *J Am Ceram Soc* 2007;**90**: 143–8.
31. Wang DN, Liang KM. The effect of carbon on the phase stability of zirconia. *J Mater Sci Lett* 1998;**17**:343–4.
32. Heuer AH, Lou VLK. Volatility diagrams for silica, silicon nitride, and silicon carbide and their application to high-temperature decomposition and oxidation. *J Am Ceram Soc* 1990;**73**:2789–803.
33. Shimada S. A thermoanalytical study on the oxidation of ZrC and HfC powders with formation of carbon. *Solid State Ionics* 2002;**149**: 319–26.
34. Zhang X-H, Hu P, Han J-C. Structure evolution of ZrB_2–SiC during the oxidation in air. *J Mater Res* 2008;**23**:1961–72.
35. Zhang JF, Wang LJ, Jiang W, Chen LD. High temperature oxidation behavior and mechanism of Ti_3SiC_2–SiC nanocomposites in air. *Compos Sci Technol* 2008;**68**:1531–8.
36. Reichle M, Kickl JJ. Investigation about the high temperature oxidation of titanium carbide. *J Less-Common Met* 1972;**27**:213–36.
37. Shimada S, Yunazar F. Oxidation of hafnium carbide and titanium carbide single crystals with the formation of carbon at high temperatures and low oxygen pressures. *J Am Ceram Soc* 2000;**83**:721–8.
38. Rao GR, Venugopal V. Kinetics and mechanism of the oxidation of ZrC. *J Alloys compd* 1994;**206**:237–42.
39. Sciti D, Silvestroni L, Guicciardi S, Fabbriche DD, Bellosi A. Processing, mechanical properties and oxidation behavior of TaC and HfC composites containing 15 vol% $TaSi_2$ or $MoSi_2$. *J Mater Res* 2009;**24**:2056–65.
40. Vaughn WL, Maahs HG. Active-to-passive transition in the oxidation of silicon carbide and silicon nitride in air. *J Am Ceram Soc* 1990;**73**:1540–3.
41. Han W-B, Hu P, Zhang X-H, Han J-C, Meng S-H. High-temperature oxidation at 1900 °C of ZrB_2–xSiC ultrahigh-temperature ceramic composites. *J Am Ceram Soc* 2008;**91**:3328–34.